Carbonates thermal decomposition kinetics and their implications in using Rock-Eval ® analysis for carbonates identification and quantification

François Baudin, Nicolas Bouton, Adrien Wattripont, Xavier Carrier

▶ **To cite this version:**

REGULAR ARTICLE

Carbonates thermal decomposition kinetics and their implications in using Rock-Eval® analysis for carbonates identification and quantification

François Baudin [iD], Nicolas Bouton[2] [iD], Adrien Wattripont[2], and Xavier Carrier[3] [iD]

[1] Sorbonne Université, CNRS, Institut des Sciences de la Terre – Paris, ISTeP, UMR 7193, 4 place Jussieu, F-75005 Paris, France
[2] Vinci Technologies, 27B rue du Port F-92000 Nanterre, France
[3] Sorbonne Université, CNRS, Laboratoire de Réactivité de Surface, LRS, UMR 7197, 4 place Jussieu, F-75005 Paris, France

Abstract. In 2014, Pillot *et al.* [Identification and quantification of carbonate species using Rock-Eval pyrolysis, *Oil Gas Sci. Technol. – Rev. IFP* **69**, 341–349. https://doi.org/10.2516/ogst/2012036] proposed to use the Rock-Eval® method as a reliable tool to identify and quantify carbonates in solid samples from the CO_2 flux emitted by their progressive thermal decomposition during programmed heating under oxidant atmosphere. Nevertheless, several phenomena associated with the thermal decomposition of carbonates were not explained by these authors. This paper attempts to explain these phenomena by adding 5 new carbonate species to the 9 studied by Pillot *et al.* https://doi.org/10.2516/ogst/2012036 and by developing a kinetic approach to the thermal decomposition of carbonates. It appears that the kinetics of thermal decomposition of most carbonates is not of order 1 but varies according to carbonate species. Consequently, the thermal decomposition temperature varies with both the sample weight and the temperature rate applied. The thermal stability of simple carbonates is explained by the electronegativity of the cations associated with the carbonate anion. Our study provides further insights into the use of Rock-Eval® for the identification and quantification of different carbonate species.

Keywords: Carbonate decomposition, Kinetics, Rock-Eval® analysis, Thermogravimetric analysis, Elemental analysis.

1 Introduction

The carbonate ion (CO_3^{2-}) is a well-defined chemical species in which the three oxygens atoms are organised in the same plane as the carbon atom at a distance of 1.30 ± 0.01 Å and with a bond angle of $120°$ [1]. The Lewis structure of the carbonate ion has two single bonds with negative oxygen atoms and one short double bond with a neutral oxygen atom. A carbonate mineral forms when a positively charged ion (M^+, M^{2+}, or M^{3+}) associates with negatively charged oxygen atoms, forming electrostatic attractions with them and giving an ionic compound, such as:

$$2M^+ + CO_3^{2-} \rightarrow M_2CO_3,$$

$$M^{2+} + CO_3^{2-} \rightarrow MCO_3,$$

$$2M^{3+} + 3CO_3^{2-} \rightarrow M_2(CO_3)_3.$$
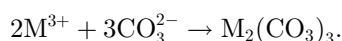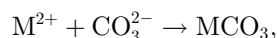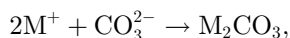
Carbonates generally decompose on heating to high temperatures, releasing carbon dioxide (CO_2) and leaving behind an oxide of the metal. This process is called calcination, after the Latin name of quicklime or calcium oxide (CaO) which is obtained by roasting limestone in a lime kiln. Indeed, all carbonates decompose thermally with a release of CO_2; the decomposition product being either the corresponding oxide or a secondary carbonate, the latter decomposing with further evolution of CO_2 as the temperature increases [2].

In 2014, Pillot *et al.* [3] proposed the use of Rock-Eval® as a reliable and rapid method to characterize and quantify carbonates in solid samples from the CO_2 flux emitted by their progressive thermal decomposition during programmed heating under ambient atmosphere. According to their work, the decomposition temperatures of 9 classical carbonate species (aragonite, azurite, calcite, dolomite, hydromagnesite, magnesite, malachite, rhodochrosite, and siderite) are sufficiently distinct to differentiate them from each other. As the authors claim "the different types of carbonates are identifiable by the temperature and the shape of the peaks (notably height and area of the peaks).

---

* Corresponding author: francois.baudin@sorbonne-universite.fr

This profile is a unique fingerprint and characterises each type of carbonate within the sample". Moreover, in the case of a mixture of carbonates, the quantification of each decomposition temperature peak gives the respective proportions of the different carbonate species in the sample. This seemingly simple method can be easily applied in a wide range of disciplines, both academic (geology, soil science) and industrial (cement and lime industry, iron smelting, ceramic glazes manufacture...).

Nevertheless, several phenomena associated with thermal decomposition highlighted in the Pillot *et al.* [3] are not explained or are incompletely elucidated. Thus, several questions remain unanswered, including:

1. Why is there an effect of sample weight on the decomposition temperature with generally an increase of temperature as weight increases, as shown in Figure 1?
2. While this effect is very marked for calcite, aragonite, dolomite and magnesite, it is not obvious for siderite and malachite whereas azurite and rhodochrosite show a small decrease in decomposition temperature with increasing weight.
3. Why do some carbonates show a stepwise decomposition while others decompose at a single temperature?

This paper attempts to answer these questions by adding 5 new carbonate species (ankerite, cerussite, huntite, nahcolite, and strontianite) to the 9 studied by Pillot *et al.* [3] and by developing a kinetic approach to the thermal decomposition of carbonates. The same analytical conditions as those employed by Pillot *et al.* [3] were applied (see Sect. 2.2.1). In order to verify that the decomposition temperatures provided by the Rock-Eval® are accurate, comparative measurements were performed by thermogravimetric analysis (TGA). To ensure that the quantification of CO_2 (from which $\%C$ is derived) by Rock-Eval® is correct, C measurements were performed by elemental analysis (EA). Our results (i) provide explanations for phenomena described by Pillot *et al.* [3], (ii) modulate some of their conclusions, and (iii) provide limitations to the use of Rock-Eval® for the identification and quantification of different carbonate species.

2 Material and methods

2.1 Material

Fourteen natural carbonates from the Sorbonne University mineral collection, as well as from colleagues' collections, were selected for this study (Tab. 1). Nine of these carbonates have been studied by Pillot *et al.* [3]. Five new carbonate species were added for our study, allowing us to broaden the spectrum of elements associated with the carbonate ion (Na, Sr, Pb), and to test carbonates with more complex chemistry, such as huntite (Mg_3Ca $(CO_3)_4$) or ankerite ($Ca(Fe, Mg, Mn)(CO_3)_2$). The thermal decomposition temperature(s) given in the literature for each of these 14 carbonates are reported in Table 1.
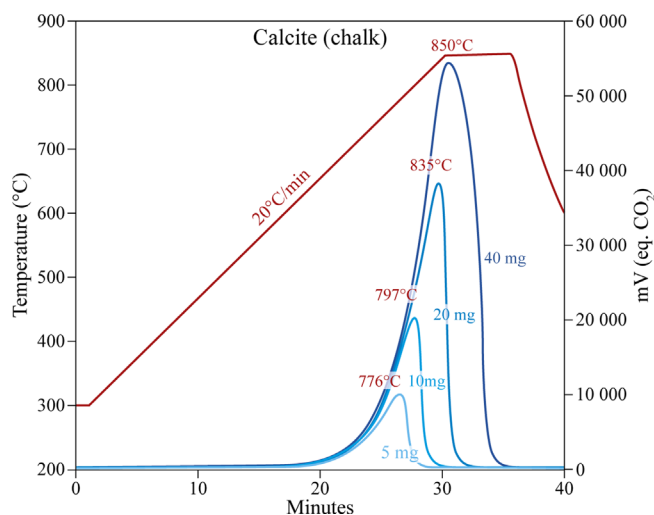

Fig. 1. Effect of the weight of a chalk sample on CO_2 production during its thermal decomposition in a Rock-Eval® 6 apparatus (modified from [3]). An increase in the temperature of the maximum CO_2 flux is evidenced by an almost 75 °C shift, from 5 to 40 mg of sample.

2.2 Methods

2.2.1 Rock-Eval® for carbonate analysis

The method described by Pillot *et al.* [3, 4] measures the CO_2 evolved by a sample when its carbonate content is thermally decomposed during a monitored heating. The method uses only the oxidation step of the Rock-Eval® [5, 6] in which the CO_2 (and CO) are continuously detected by an infrared spectrometer. Approximately 40 mg of the sample are heated following a programmed temperature ramp of 20 °C min^{-1} in the oxidation oven of the Rock-Eval® flushed with a continuous flow of 100 ml min^{-1} of dry and CO_2-free ambient air. The oxidation oven of the Rock-Eval® 6 device heats in the range of 100–850 °C [5, 6] whereas, for the Rock-Eval® 7 device, the heating starts at room temperature (+20 °C), and may reach up to 1200 °C [7–9].

For this study, the Rock-Eval® measurements were performed using both Rock-Eval® 6 and Rock-Eval® 7 devices at Institut des Sciences de la Terre (Paris). Some analyses were duplicated to check the reproducibility of the results, which is excellent with a standard deviation of ±2 °C on the temperature determination and ±0.05% on the C content. Because the purpose of our study is to elucidate the origin of the mass effect, we have analyzed the different carbonate species with weights ranging from 2 to 60 mg. For the kinetic purpose, we have analyzed calcite and siderite using different heating ramps, namely 2, 5, 20 and 30 °C min^{-1}.

2.2.2 Thermogravimetric analysis

Thermogravimetric analysis or thermal gravimetric analysis (TGA) is a method of thermal analysis in which the change of the mass of a sample is measured over time as the temperature increases [10]. This measurement provides

Table 1. Name, source collection, origin, chemical formula, molecular weight, theoretical carbon content (in %wt) and known decomposition temperature (in °C) of the 14 carbonate species considered in this study. Coll.: FB: François Baudin, KB: Karim Benzerara, LLC: Laurence Le Callonnec, MdR: Marc de Rafélis, SM: Salomé Mignard, SU: Sorbonne University.

Mineral species	Coll.	Origin (Country – Site)	Formula	Mol. weight	Theoretical %C	Decomposition temperature (°C)
Ankerite	SU	Italy – Traversella	$Ca(Fe, Mg, Mn)(CO_3)_2$	206	11.7	nd
Aragonite[*]	SU	Morroco – Tasouta	$CaCO_3$	100	12.0	~800
Azurite[*]	SU	Morroco	$Cu_3(CO_3)_2(OH)_2$	344	7.0	~400
Calcite[*]	LLC	Iceland	$CaCO_3$	100	12.0	~800
Cerussite	SU	Congo	$PbCO_3$	267	4.5	315
Dolomite[*]	SU	Spain – Eugui	$CaMg(CO_3)_2$	184	13.0	~800
Huntite	SM	Comoros – Dziani Lake	$Mg_3Ca\ (CO_3)_4$	353	13.6	nd
Hydromagnesite[*]	KB	Iran – Soghan	$Mg_5(CO_3)_4(OH)_2\ 4H_2O$	468	10.3	220–550
Magnesite[*]	SU	Brazil – Brumado	$MgCO_3$	84	14.3	350
Malachite[*]	LLC	Congo	$Cu_2CO_3(OH)_2$	221	5.4	nd
Nahcolite	FB	?	$NaHCO_3$	84	14.3	~100
Rhodochrosite[*]	SU	South Africa	$MnCO_3$	115	10.4	nd
Siderite[*]	SU	Greenland	$FeCO_3$	116	10.3	~500
Strontianite	MdR	Scotland – Strontian Mine	$SrCO_3$	148	8.1	>1200

[*] Species studied by Pillot *et al.* (2014); nd: no data.

information about physicochemical phenomena, such as phase transitions, absorption, adsorption, desorption, thermal decomposition, and solid–gas reactions (*e.g.*, oxidation or reduction). TGA measurements were performed using an SDT (TGA/DSC) Q600 (TA Instruments) apparatus at Laboratoire de Réactivité de Surface (Paris). The setting of the machine was as close as possible to that of the Rock-Eval®, namely a temperature ramp of 20 °C min^{-1} and sweeping of the oven with an 80/20 N_2/O_2 mixture at a flow of 100 ml min^{-1}. For this study, only the weight changes related to the thermal decomposition of the different carbonate species were compared to those obtained with the Rock-Eval® method. The weight change is here expressed as the derivate weight in % °C^{-1}, which is the most comparable signal to those of the evolved CO_2, given by the Rock-Eval®.

2.2.3 Elemental analysis

Elemental analysis (EA) was conducted on all selected carbonate species using a FLASH 2000 analyzer (Thermo Scientific) at Institut des Sciences de la Terre (Paris). The apparatus operates according to the dynamic flash combustion of the sample for the determination of carbon, hydrogen, nitrogen and sulfur. Approximately 6 mg of each carbonate sample was weighed in a tin capsule and introduced by an autosampler into the combustion reactor, heated at 960 °C. When the sample enters the reactor, a small volume of pure oxygen is added to the system and helps to burn the material, converting the sample into elemental simple gases, including CO_2. A separation column and thermal conductivity detector allow us to determine C concentrations in the sample with a ±0.05% precision. Every sample was analyzed in triplicate.

3 Some reminders on kinetic

Considering a chemical reaction R(eagent) → P(roduct), the rate of production of P, V_P, is equal to the opposite of the rate of consumption of R, V_R:

$$V_P = V_R = \frac{d[P]}{dt} = -\frac{d[R]}{dt}$$

with $[R]$ the concentration or mass of R, which decreases as the reaction proceeds, and $[P]$ the concentration or mass of P, which increases with time. According to Arrhenius and Boltzmann, this rate is written as follows:

$$\frac{d[P]}{dt} = A \times e^{\frac{-Ea}{RT}} \times [R]_t,$$

where t, time, in seconds; A, Arrhenius factor (or pre-exponential factor, corresponding to unimolecular reactions to typical vibrational frequencies of the molecular bonds [11]), in s^{-1}; T, the temperature, in K; R, the perfect gas constant, 8.314 J · mol^{-1} · K^{-1}; $[R]_t$, the concentration of reagent remaining to be transformed at each time t. The energy, in two forms, is the chemical activation energy, necessary to initiate the reaction, Ea, in J · mol^{-1}, and RT, in J · mol^{-1}, which is the thermal energy given to the reaction system.

The numerical solution of this differential equation gives a Gaussian curve. This reaction is called order 1, because:

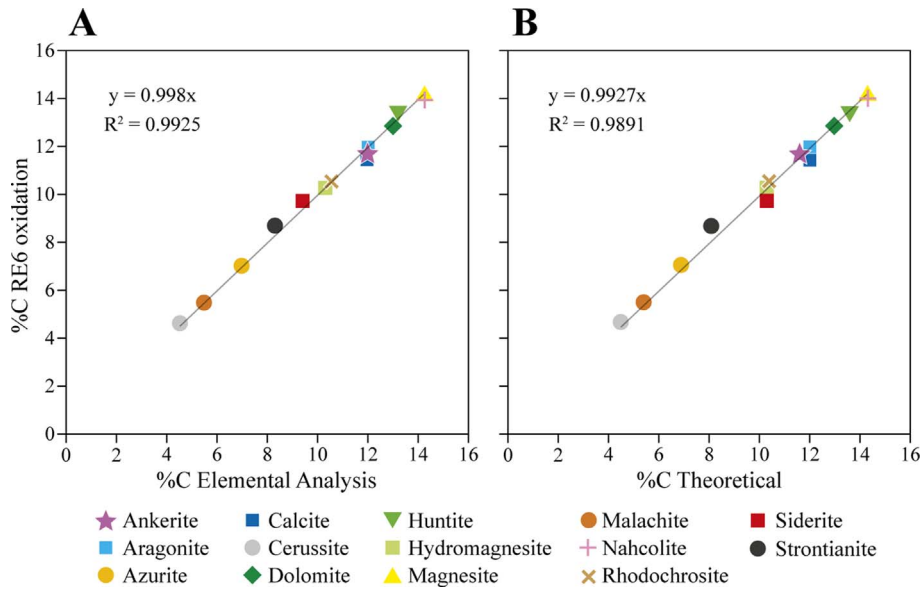$$\frac{d[P]}{dt} = A \times e^{\frac{-Ea}{RT}} \times [R]^1.$$

A

B

Fig. 2. (A) Comparison of the carbon concentration (wt%) for 14 species of carbonates measured by the Rock-Eval® method (RE oxidation) with the measurements made by elemental analysis. (B) Comparison of the carbon concentration (wt%) for 14 species of carbonates measured by the Rock-Eval® method with the theoretical C content given in Table 1.

If a chemical reaction involved two molecules of R to produce one molecule of P, the resolution of the Arrhenius equation would be the following:

$$\frac{\mathrm{d}[P]}{\mathrm{d}t} = A \times e^{\frac{-Ea}{RT}} \times [R]^2.$$

This equation is then said to be of order 2, in reference to the term $[R]$.

The decomposition kinetics of solids is sometimes described as being of order $n = 0$. In that case, the equation is:

$$\frac{\mathrm{d}[P]}{\mathrm{d}t} = A \times e^{\frac{-Ea}{RT}} \times [R]^0.$$

The term of the quantity of reagent still to be transformed disappears, the equation is no longer differential and finally becomes:

$$\frac{\mathrm{d}[P]}{\mathrm{d}t} = A \times e^{\frac{-Ea}{RT}}.$$

The reaction takes place only under the effect of time and temperature and stops when the reagent is consumed. The shape of the curve is no longer Gaussian, but purely exponential, and suddenly falls to zero when the reagent is finally consumed. So, during non-isothermal experiments, the more reagents to consume, the more time and temperature the reaction takes.

There are, in fact, reactions of order n, where n can be any number, usually $n > 0$. When one doesn't observe 1 or 2 order kinetics it means that the transformation consists of a series of elementary reactions [11]. Then the equation can be generalised and written as:

$$Q^{'}(t) = -Ae^{\frac{-Ea}{RT}}Q(t)^n \qquad (1a)$$

and

$$Q(t) = Q_0 - \int_{t=0}^{t} Q'(t) \qquad (1b)$$

with $Q(t)$ the concentration or mass of reactant at time t, and Q_0 the initial quantity of sample at the start of the reaction (at $t = 0$).

4 Results

4.1 Carbon content accuracy

The determination of the carbon content of the 14 studied samples by the Rock-Eval® carbonate method is excellent when compared with that obtained by elemental analysis. As shown in Figure 2, the data points are distributed in a binary diagram near the 1:1 line with an R correlation coefficient greater than 0.99. The comparison of the Rock-Eval® measurements with the theoretical values given in Table 1 is also excellent even if we note a very slight decrease in the correlation coefficient which is just below 0.99. The weaker correlation between the analytical techniques and expected value is certainly due to the chemical composition of certain of our samples which deviates from the model chemical compound.

4.2 Kinetic effects on calcite and siderite decomposition

The heating rate has a strong influence on the decomposition temperature, as shown by the results of the decomposition of 40 mg of calcite with increasing temperature ramps of 2, 5, 20 and 30 °C min⁻¹ (Fig. 3). According to Rock-Eval® measurements, the temperature of the maximum CO_2 release varies from 675 °C to 790 °C with the increasing
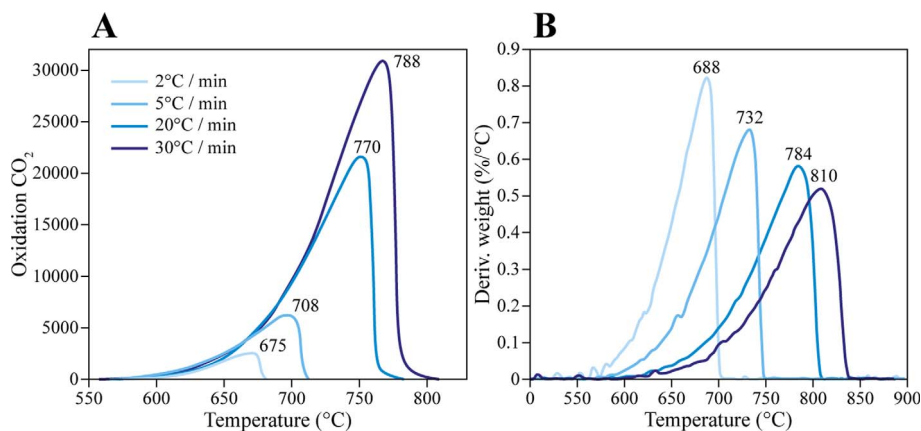
Fig. 3. Evidence of a kinetic effect during the thermal decomposition of 40 mg of pure calcite decomposed with temperature gradients ranging from 2 to 30 °C min^{-1}. (A) Result with the Rock-Eval$^{®}$ expressed in equivalent CO_2 as a function of the oven temperature. (B) Result of the TGA measurements expressed as a derivate of the weight as a function of the oven temperature. An increase in the maximum decomposition temperature is observed with increasing heating ramps.

heating ramps (Fig. 3A), *i.e.* a difference of 115 °C. The same experiment with TGA shows temperature variation in the same range, 688–810 °C, and a similar absolute difference of Ca, 120 °C (Fig. 3B). The slight difference in temperature between the two methods is certainly linked to the temperature calibration of both instruments.

It can be noted that whatever the temperature ramp, the thermal decomposition of calcite always begins at 575 °C (Fig. 3A). The weight of the analyzed sample has no effect on this initial thermal decomposition temperature as can be seen in Figure 1.

By contrast, the decomposition of 40 mg of siderite with the same increasing temperature ramps (2, 5, 20 and 30 °C min^{-1}) does not show the same kinetic effect as for calcite. According to the Rock-Eval$^{®}$ analysis, the decomposition temperature difference is less than 30 °C, from 508 to 537 °C (Fig. 4). Moreover, the peak shape of siderite (Fig. 4) is more Gaussian than the peak shape of calcite (Fig. 3A). The displacement of the peaks is sometimes referred to be due to mass transfer or heat transfer.

4.3 Decomposition thermograms of selected carbonates

The Rock-Eval$^{®}$ signals of 9 pure carbonate species reported by Pillot *et al.* [3] are here completed with those of cerussite, huntite, ankerite and strontianite. The shape and temperature(s) of the maximal decomposition of 13 carbonate species are shown in Figure 5A. Cerussite ($PbCO_3$) decomposes at low temperatures (≤400 °C) with a two-step reaction, the first one with a maximum near 340 °C and the second near 400 °C. Huntite ($Mg_3Ca (CO_3)_4$) decomposition displays also a two-step reaction, the first one with a maximum near 600 °C and the second one near 800 °C. Ankerite ($Ca(Fe, Mg, Mn)(CO_3)_2$) decomposes with a signal very similar to that of calcite/aragonite. Strontianite ($SrCO_3$) decomposes at high temperature (>850 °C) and need the use of Rock-Eval$^{®}$ 7 to be analyzed. It decomposes in two steps with smooth curves. The first step maximizes near 1000 °C and the second near 1100 °C. Rock-Eval$^{®}$ (Fig. 5A) and TGA (Fig. 5B) signals are very similar both
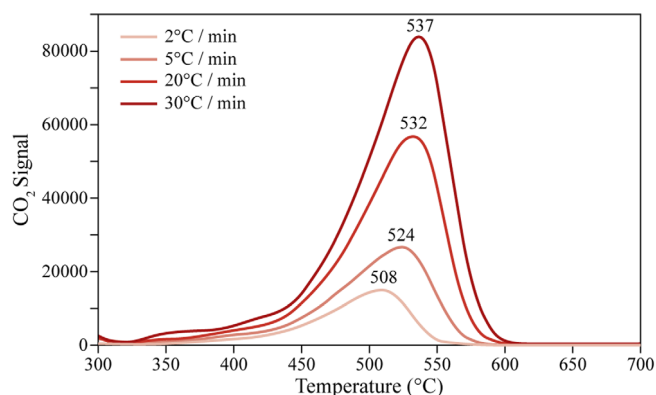

Fig. 4. Low kinetic effect during the thermal decomposition of 40 mg of pure siderite decomposed with temperature gradients ranging from 2 to 30 °C min^{-1} using Rock-Eval$^{®}$, compared to calcite (cf Fig. 3).

for shape and temperature(s) of decomposition for every carbonate species. However, some difference appears using TGA, such as (i) a lower rhodochrosite decomposition temperature, (ii) the disappearance of the third decomposition peak for hydromagnesite and (iii) a narrower decomposition range for strontianite. Note that cerussite was not analyzed using TGA for safety reasons (to prevent leaded vapours).

Some differences also appear within the Rock-Eval$^{®}$ signals between Pillot *et al.*'s and ours. Our rhodochrosite sample decomposes between siderite and magnesite, whereas in Pillot *et al.* it decomposes after magnesite (see Fig. 1 of Pillot *et al.* [3] and compare with Fig. 5A, here). Our azurite sample shows a two-step decomposition whereas in Pillot *et al.* it decomposes in a single reaction (see Fig. 2 of Pillot *et al.* [3]).

4.4 Mass effect

Pillot *et al.* [3] observed a sample mass effect characterised by a shift of temperature of the maximal release of CO_2. Its amplitude depends on the different carbonate types. It is
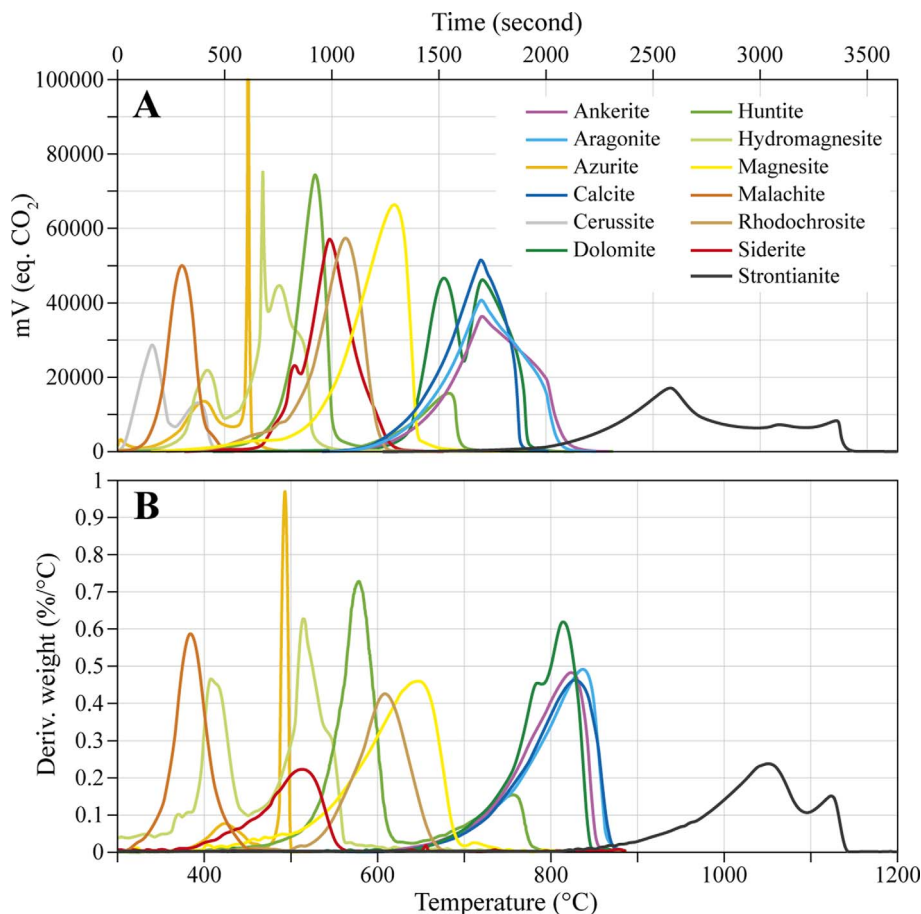
Fig. 5. (A) Distribution of Rock-Eval® signal for 13 carbonate species analyzed in oxidation step alone (with a 20 °C min^{-1} heating rate) using 40 mg of sample. Strontianite was analyzed with a Rock-Eval® 7 apparatus to reach temperatures >900 °C at which it decomposes, while the other carbonates were analyzed with Rock-Eval® 6 apparatus. (B) Comparison of TGA signal for 12 carbonate species using the same analytical conditions as for the Rock-Eval®. Cerussite was not analyzed using TGA because of safety reasons.

more pronounced for small weight and tends to disappear for most carbonate around 40 mg. Our study confirms this effect and completes the data of Pillot *et al.* [3] with 5 new species of carbonates (Fig. 6).

For the new carbonate species analyzed, the mass effect has an influence beyond 40 mg on the second peak of decomposition of strontianite and huntite. For cerussite, the plateaus for both peaks do not seem to be reached with 40 mg. Analyses with higher weights would have been necessary but for safety reasons (prevention of leaded vapors) these analyses were not carried out.

5 Discussion

In order to answer the initial questions raised in the introduction (*i.e.* why the temperature at the maximum of the thermal decomposition depends both on the type of carbonate and on the weight of the sample), the Arrhenius equation is derived to study the effect of the order of reaction n on the decomposition curves, as well as the effect of the initial weight of carbonate. Mathematically, it is indeed

possible to describe and predict the effect of the initial weight, depending on the order of reaction n. Numeric simulations of these curves can also be plotted to compare with experimental data.

5.1 Carbonate thermal decomposition follows kinetic order *n*

As recalled in Section 3, the decomposition kinetics may have different order values: n. According to Roduit [12], the decomposition reaction of calcite ($CaCO_3 \rightarrow CaO + CO_2$) is of order $n = 0.177$; that is not quite equal to zero, but far from 1.

The temperature at which the maximum CO_2 yield is observed (that is called T_{peak} in Rock-Eval® methodology) corresponds to the maximum of the $Q'(t)$ curve. Since the temperature profile is not isothermal, but the temperature increases with a constant heating rate, called β, in °C min^{-1}, the temperature $T(t)$ is written as:

$$T(t) = T_0 + \beta t$$

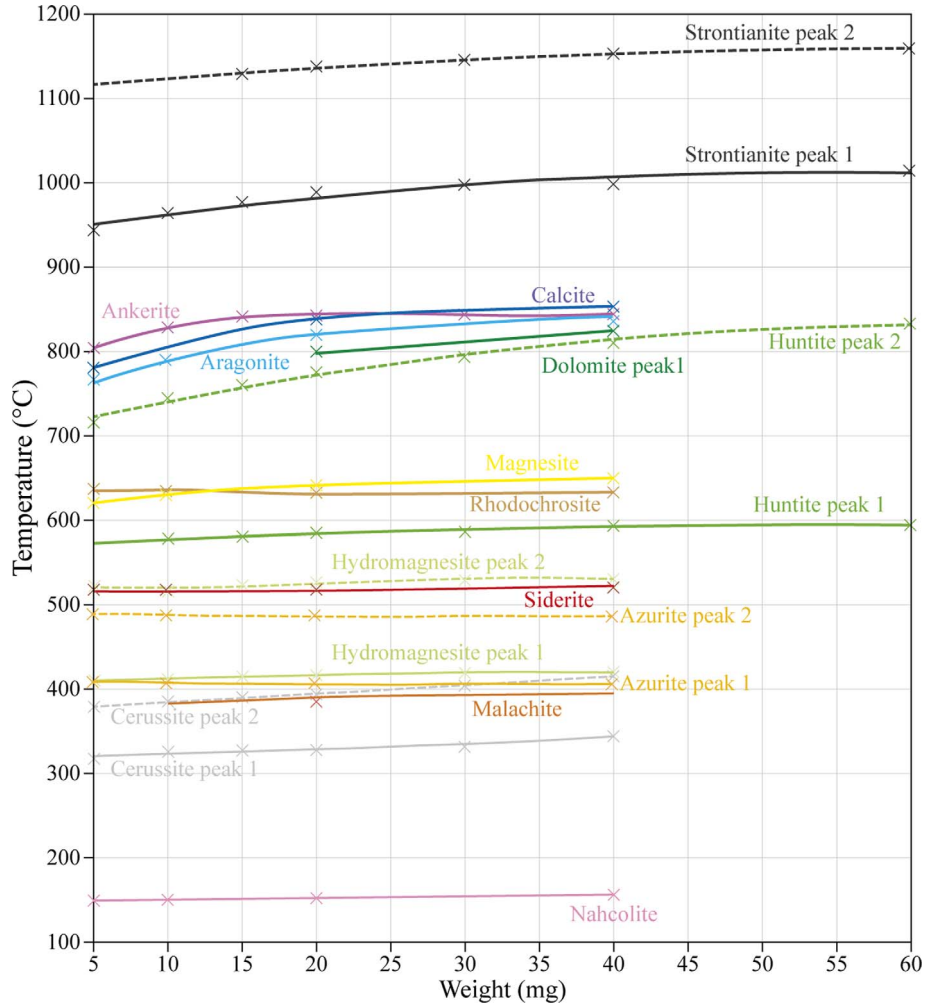with $T_0 \geq i_0$ and $\beta \geq t_0$.

Fig. 6. Effect of the weight of the sample on the temperature of the maximum CO_2 production during the decomposition of different carbonates by the Rock-Eval® method.

When derivating equation (1a)

$$Q''(t) = -A\frac{Ea\beta}{RT(t)^2}e^{-\frac{Ea}{RT}}Q(t)^n - Ae^{-\frac{Ea}{RT}}nQ(t)^{n-1}Q'(t),$$

$$Q''(t) = \left(\frac{Ea\beta}{RT(t)^2} + n\frac{Q'(t)}{Q(t)}\right)Q'(t). \tag{2}$$

At the T_{peak} point, corresponding to time $t = tp$, the decomposition curve $Q'(t)$ is at its maximum, so that the derivative of the $Q'(t)$ is thus equal to zero:

$$Q''(t_p) = 0,$$

$$\frac{Ea\beta}{RT(tp)^2} + n\frac{Q'(tp)}{Q(tp)} = 0.$$

Which leads to:

$$\frac{Q'(tp)}{Q(tp)} = -\frac{Ea\beta}{nRT(tp)^2}. \tag{3}$$

Moreover, from equation (1) one get equation (4) below:

$$-\frac{Q'(tp)}{Q(tp)^n} = Ae^{-\frac{Ea}{RT(tp)}}. \tag{4}$$

By injecting (4) in (3), one get:

$$\frac{1}{n}\frac{Ea\beta}{RT(tp)^2}\frac{1}{Q(tp)^{n-1}} = Ae^{-\frac{Ea}{RT(tp)}}.$$

Leading to equation (5):

$$Q(tp)^{(n-1)} = \frac{Ea\beta}{nRAT(tp)^2}e^{\frac{Ea}{RT(tp)}}. \tag{5}$$

If $n = 1$, then

$$\frac{Ea\beta}{ART(tp)^2}e^{\frac{Ea}{RT(tp)}} = 1$$

or

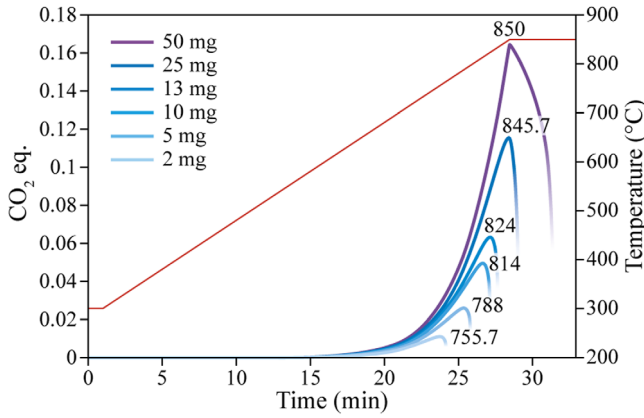$$\frac{Ea\beta}{ART(tp)^2} = e^{\frac{-Ea}{RT(tp)}}. \tag{6}$$

Fig. 7. Simulations of the Rock-Eval® CO$_2$ curve for increasing weights (concave index) and for order $n = 0.177$ (Tp increases as the weight increases), that simulate the actual experimental curve shapes shown in Figure 1, based on equations (1a) and (1b).

That leads to the so-called Kissinger equation (also known as ASTM E2890-21 [13]).

$$\ln\left(\frac{\beta}{Tp^2}\right) = \ln\left(\frac{AR}{Ea}\right) - \frac{Ea}{RTp} \quad (7)$$

for $n = 1$ that allows to predict A and Ea values based on several non-isothermal analyses of the same sample.

If supposing $n \neq 1$, a new function is introduced in order to study the comportment of equation (5), g_n defined for $x > 0$ by:

$$g_n(x) = \left(\frac{e^{\frac{1}{x}}}{x}\right)^{\frac{1}{n-1}}. \quad (8)$$

From equation (5), can be deduced:

$$Q(tp) = \left(\frac{\beta R}{nAEa}\right)^{\frac{1}{n-1}} g_n\left(\frac{RT(tp)}{Ea}\right). \quad (9)$$

Also, in order to know the trend of equation (9), how $Q(tp)$ behaves in function of $T(tp)$, or how Tp is dependent on $Q(tp)$, it is sufficient to study the function g.

– if $n > 1$, $g'_n < 0$ on $]0; +\infty[$, thus g_n is strictly decreasing on $]0; +\infty[$, and g_n^{-1} is also strictly decreasing, since $(g_n^{-1})' = \frac{1}{g'_n \circ g_n^{-1}}$
– if $0 < n < 1$, $g'_n > 0$ on $]0; +\infty[$, thus g_n is strictly increasing on $]0; +\infty[$, and g_n^{-1} is also strictly increasing

When studying mathematically these functions, it is finally possible to conclude that:

– if $n = 1$, Tp is not dependent on the quantity of sample in the crucible (*cf.* Eq. (7)),
– if $n < 1$, Tp increases with $Q(tp)$, and thus with the initial weight, Q_0, in the crucible,
– if $n > 1$, the Tp decreases when $Q(tp)$ increases, thus when the initial weight of sample in the crucible increases.

Considering that calcite decomposition follows $n = 0.177$ according to Roduit [12], the peak shapes of Figure 1 are now fully understood when increasing the weight of the sample to be decomposed. The peaks can even be numerically calculated, and the obtained curves (Fig. 7) predict indeed the behaviour observed in experimental data of Fig. 1: T_{peak} increases with initial weight. The effect of temperature gradients on T_{peak} can also be understood and calculated for calcite and siderite: as n decreases the effect of the gradient on T_{peak} is more pronounced.

Also, when the weight of calcite to be decomposed increases, the peak is deformed mostly on the high-temperature side. The mathematical description of this peak displacement due to the weight and due to n is discussed in Appendix A in detail.

Mass transfer and heat transfer are physical phenomena that do take place in the volume of the bulk sample but are not the one and only reason for this peak displacement with initial mass that undergoes the decomposition phenomena. When analyzing a IFPEN 160,000 reference sample, containing some calcite among other compounds, the heat and mass transfer within the sample cannot be sufficient to describe the displacement of peak shapes due to the initial mass only, as seen in Figures 8A and 8B.

When the weight of the rock to be decomposed increases the peak in Figure 8B spreads quite evenly on the low and high-temperature sides than the peak of calcite in Figure 8A, where the peak is deformed mostly on the high-temperature side and does not show a symmetrical Gaussian shape, whereas heat and mass transfer occur for all parts of the rock. The mathematical reason for this peak shape displacement is discussed above, as well as in Appendix A in detail.

5.2 A thermal stability scale of simple carbonates

Figures 5 and 6 clearly demonstrate that the thermal stability of studied carbonate covers a wide range of temperatures, extending over almost 1000 °C, from nahcolite (150 °C) to strontianite (1150 °C for its second decomposition peak). As a first approximation, Pillot *et al.* [3] mentioned that "copper carbonates are decomposed first, then iron carbonates, then manganese carbonates, then magnesium carbonates, then finally calcium carbonates". It is clear that the thermal decomposition temperature of simple carbonates strongly depends on the cations (M^{2+}) associated with the carbonate anion (CO$_3^{2-}$), and more precisely on their electronegativity. The lower the electronegativity of the cation, the higher the decomposition temperature or, in other words, the stronger the energy binding the cation to the carbonate anion. Thus, for Ca, Mn, Fe and Cu (four elements of the 4th period of the periodic table), the electronegativity increases respectively from 1 to 1.55 then to 1.83 and finally to 1.9 (in the Pauling scale), hence a decrease in the decomposition temperature going from calcite to rhodochrosite, to siderite and finally to azurite. For the same group of the periodic table (same column of the periodic table), the electronegativity tends to decrease as the atomic number increases. Thus, for the Mg, Ca and Sr succession of the 2nd group, the
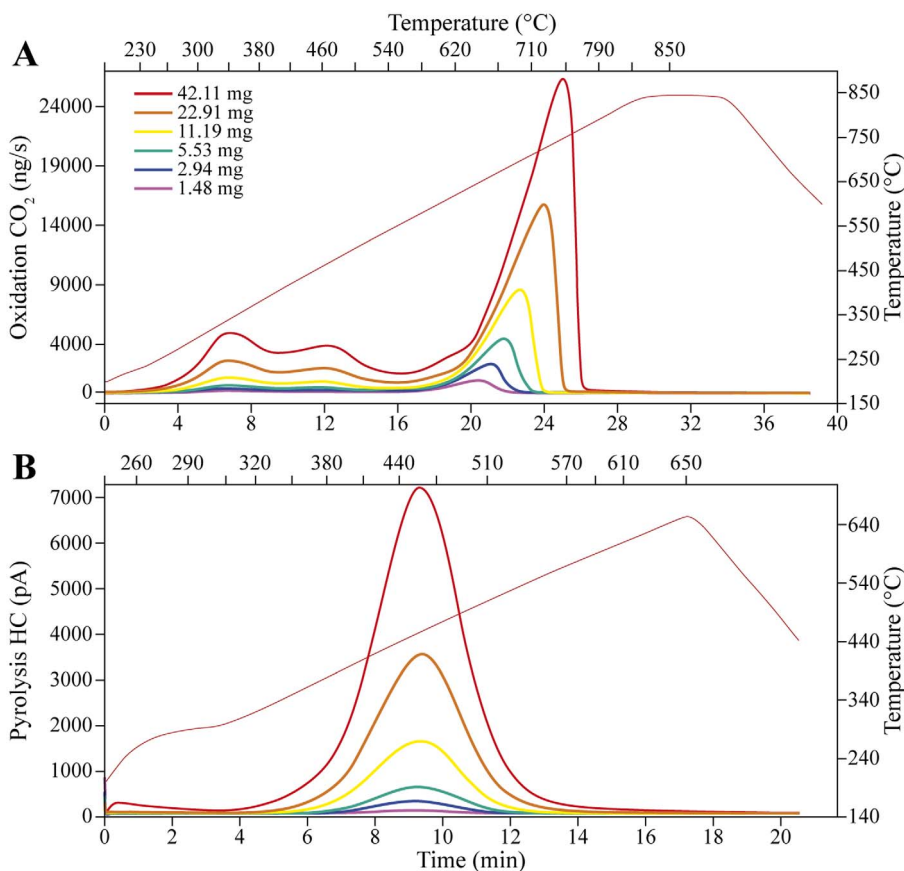
Fig. 8. (A) Rock-Eval CO_2 signal (oxidation phase) of increasing weights of the same sample: the peak on the right-side signs for calcite decomposition, while the peaks on the left side are the signature of the combustion of the organic matter trapped into the rock. (B) Rock-Eval FID signal (pyrolysis phase) of increasing weights of the same sample: the peak area increases in the evenly distributed manner toward low and high temperature, but T_{peak} remain constant, which is an indication of order 1 decomposition of organic matter reaction.

electronegativity value decreases from 1.31 to 1.00 then falls to 0.95, hence an increase in the decomposition temperature going from magnesite to calcite, and finally to strontianite.

In addition, the lower the electronegativity of the cations, the greater the effect of weight on the decomposition temperature. This is explained by thermal decomposition kinetics tending towards a zero-order as the electronegativity decreases. The numerical resolutions of the kinetics of order 1 do not show any change of curve according to the initial weight, whereas the more the order of reaction tends towards 0, the more the effect of the weight is marked on the temperature of decomposition, and the more concave the shape of the peak on the final temperature plateau (Fig. 7). The final shape of the thermogram is, therefore, a visual index of percentage decomposition.

Figure 9 consists of a plot of thermal decomposition temperature *versus* the electronegativity values of the cations implicated in simple carbonates studied here. The stability decrease appears to be an exponential relationship.

The remark of Pillot *et al.* [3] about a chemical relationship explaining the carbonate's thermal stability finds its logical explanation here. Then, it remains to explain

why some carbonates decompose with a single CO_2 release peak while others show two or even three decomposition peaks.

5.3 The causes of a decomposition in one or more steps

According to Pillot *et al.* [3], simple carbonates (such as siderite, magnesite, rhodochrosite, calcite and aragonite) and simple carbonates linked with hydroxide anions (such as malachite and azurite) show a single decomposition step, whereas complex carbonates of several elements (such as dolomite) show several decomposition steps. Hydrated carbonates (such as hydromagnesite) show several steps. These assertions should be modulated in the light of our results.

If simple carbonates (associating a single cation to the carbonate anion) generally exhibit a single CO_2 release peak, this is not a general rule. Cerussite ($PbCO_3$) and strontianite ($SrCO_3$), studied here, are exceptions as their thermal decomposition takes place in two steps (Fig. 5). The causes of this splitting of CO_2 release from these simple carbonates are probably different. For cerussite, its thermal decomposition led the carbonate and its oxide to interact
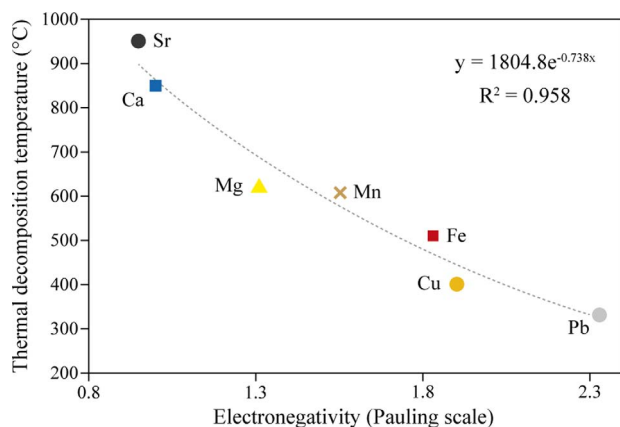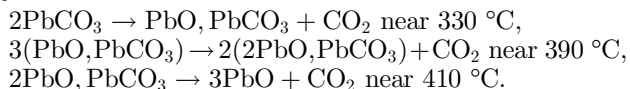
Fig. 9. Variation of the thermal decomposition temperatures of simple carbonates obtained using Rock-Eval® with the electronegativity value of the associated cation.

during the decomposition reaction, thus causing a multi-step decomposition. According to Webb and Krüger [14], the reactions are as follows:

$2PbCO_3 \rightarrow PbO, PbCO_3 + CO_2$ near 330 °C,
$3(PbO, PbCO_3) \rightarrow 2(2PbO, PbCO_3) + CO_2$ near 390 °C,
$2PbO, PbCO_3 \rightarrow 3PbO + CO_2$ near 410 °C.

These last two reactions take place at close temperatures, they generate a single CO_2 release peak during the Rock-Eval® analysis.

For strontianite ($SrCO_3$), the reason for a double peak decomposition is less clear and two explanations are possible [14]. The first is crystallographic in the case of pure strontianite. During heating, a structural change from the orthorhombic crystallographic system to the hexagonal system occurs at around 1000 °C with an initial release of CO_2 generating the first peak. Then, total decarbonation occurs around 1150 °C, generating the second peak. An alternative explanation is a chemical. As most strontianites are $CaCO_3$–$SrCO_3$ solid solutions, the two peaks can be related to a release associated with each of the two cations in the case of non-pure strontianite.

Simple carbonates linked with hydroxide anions do not show always a single decomposition step, as stated by Pillot *et al.* [3]. The azurite and malachite samples they analyzed show a single peak whereas our azurite sample yields CO_2 in two steps (Fig. 5). This two-step reaction for azurite satisfies to literature data. Indeed, Brown *et al.* [15] studied the thermal decomposition of both copper carbonates using TGA and evolved gas analysis (EGA) and showed that malachite decomposes at a single step near 380 °C whereas azurite decomposes in a two-step reaction. Brown *et al.* [15] proposed the following decomposition reactions:
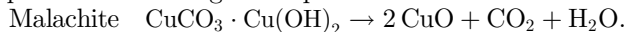
Malachite $CuCO_3 \cdot Cu(OH)_2 \rightarrow 2\,CuO + CO_2 + H_2O$.
Azurite $2CuCO_3 \cdot Cu(OH)_2 \rightarrow 1/2\big[2CuCO_3 \cdot Cu(OH)_2\big] + 3/2CuO + CO_2 + 1/2H_2O$ at a first step. In the second step, the remaining half of azurite would decompose with the same equation.

For mixed carbonates such as dolomite ($CaMg(CO_3)_2$) and huntite ($Mg_3Ca(CO_3)_4$), it is logical that the thermal decomposition between the carbonate anion and Mg and Ca cation determines a double peak as stated by Pillot

et al. [3]. The $MgCO_3$ bond cracks at a lower temperature than the $CaCO_3$ bond due to an electronegativity going from 1.31 for Mg to 1 for Ca (see Sect. 5.2 above for the explanation). On the other hand, we do not observe several peaks for ankerite whereas theoretically the elements Ca, Fe, Mg and Mn can be present in its composition. The fact that Ca largely dominates over the other cations probably explains this behaviour.

All these small differences between the results of Pillot *et al.* [3] and ours as well as the complexity of the thermal decomposition reactions of certain carbonates call for caution in the use of the Rock-Eval® method for the identification and quantification of carbonates.

5.4 Some tips on the use of Rock-Eval® for carbonate identification and quantification

The analysis of the decomposition of 14 species of carbonate shows that several CO_2 release peaks are superimposed (Figs. 5 and 6), which makes their differentiation difficult. Moreover, with the mass effect (see Sect. 4.4) and because the presence of small impurities or salt has an influence on the position of the decomposition temperature [16, 17], it becomes really difficult to characterize a mixture of carbonate species using Rock-Eval®.

If the distinction of carbonate types is not easy with the Rock-Eval® method, their quantification is an even more complex question when several species are mixed. According to Pillot *et al.* [3], in the case of a mixture of two carbonate species in a sample, the quantification of each CO_2 peak by Rock-Eval® gives the respective proportions of each species. This has been verified by these authors for synthetic magnesite–calcite and natural magnesite–dolomite mixtures. However, it should be noted that these types of mixtures are rather rare in nature. However, the Rock-Eval method is more difficult to apply to calcite–dolomite or calcite–magnesian calcite mixtures, which are the most common in nature. Indeed, the decomposition peaks of calcite and dolomite overlap using Rock-Eval, making it virtually impossible to quantify each of these species. An additional difficulty arises if the sample contains organic matter with certain types of carbonate. Indeed, hydromagnesite, azurite and siderite decompose in the temperature range where CO_2 of organic origin is generally released. In this case, it becomes very difficult to deconvolute in the CO_2 signal the part which comes from the oxidation (or pyrolysis) of organic matter from that which comes from the decomposition of carbonates [18, 19]. Despite these difficulties, it should be mentioned that, in all cases, total carbon quantification by Rock-Eval® remains valid, whatever the carbonate species encountered in the sample.

6 Conclusions

In a seminal paper, Pillot *et al.* [3] proposed to use the oxidation step of the Rock-Eval® method as a reliable tool for carbonates identification and quantification. Several phenomena highlighted by these authors have found answers with our study, namely:

- The kinetics of the thermal decomposition of all carbonates is not of order 1 like that of the thermal decomposition of kerogens but is variable according to the type of carbonate. One of the consequences is that the decomposition temperature is strongly dependent on the weight of the sample analyzed, which is not the case for kinetics of order 1. Thus, this mass effect can lead to temperature decomposition varying up to 100 °C. As one cannot know *a priori* in a natural sample the proportion of a type of carbonate, it becomes difficult to identify carbonate on the sole basis of the decomposition temperature.
- In a first approximation, we explain the thermal stability order of simple carbonates by the electronegativity of the cations associated with the carbonate anion.
- The stepwise decomposition of certain carbonates cannot be explained by a univocal cause. Multi-steps depend on physical (crystallographic changes) or chemical reactions between the carbonate and its thermal degradation product during heating.

Finally, the approach proposed by Pillot and co-authors, excluding the pyrolysis phase of the Rock-Eval® method, is not suitable for routine analysis in the petroleum industry where the "bulk rock" method is used to simultaneously quantify an organic fraction and a carbonated fraction. Nevertheless, the carbonate method proposed by Pillot *et al.* [3] has some interest in the cement industry and it has had the merit of opening up a field of research on the analysis of carbonates by the Rock-Eval® method.

Author contributions

François Baudin: Conceptualization, Resources, Methodology, Visualization, Investigation, Data curation, Supervision, Writing – original draft. Nicolas Bouton: Formal analysis, Investigation, Visualization, Writing – reviewing & editing. Adrien Wattripont: Investigation, Writing – reviewing & editing. Xavier Carrier: Resources, Writing – reviewing & editing.

Conflict of interest

The authors declare that they have no known competing financial interests or personal relationships that could have appeared to influence the work reported in this paper.

Data availability

Data will be made available on request.

References

1 Adler H.H., Kerr P.F. (1963) Infrared spectra, symmetry and structure relations of some carbonate minerals, *Am. Mineral.* **48**, 7–8, 839–853.

2 Stern K.H., Weise E.L. (1969) *High temperature properties and decomposition of inorganic salts, part 2. Carbonates*, vol. **30**, National Bureau of Standards, NSRDS-NSB, 27 p.

3 Pillot D., Deville E., Prinzhofer A. (2014) Identification and quantification of carbonate species using Rock-Eval pyrolysis, *Oil Gas Sci. Technol. – Rev. IFP* **69**, 341–349. https://doi.org/10.2516/ogst/2012036.

4 Pillot D., Deville E., Prinzhofer A. (2011) *Méthode pour la caractérisation et la quantification rapides des carbonates d'un matériau solide*, French Patent (INPI) : Brevet déposé à l'Institut National de la Propriété Industrielle le 18 mars 2011, référence n 11/00.841.

5 Lafargue E., Marquis F., Pillot D. (1998) Rock-Eval 6 applications in hydrocarbon exploration, production and soil contamination studies, *Oil Gas Sci. Technol. – Rev. IFP* **53**, 421–437. https://doi.org/10.2516/ogst:1998036.

6 Behar F., Beaumont V., De B., Penteado H.L. (2001) Rock-Eval 6 technology: performances and developments, *Oil Gas Sci. Technol. – Rev. IFP* **56**, 111–134. https://doi.org/10.2516/ogst:2001013.

7 Lamoureux-Var V., Espitalié J., Pillot D., Bouton N., Garcia B., Antonas A., Aboussou A., Wattripont A., Ravelojaona H., Noirez S., Beaumont V. (2019) Rock-Eval 7S: technology and performance, in: *29th International Meeting on Organic Geochemistry (IMOG 2019)*, Gothenburg, Sweden. https://doi.org/10.3997/2214-4609.201902941.

8 Lamoureux-Var V., Bouton N., Espitalié J., Benoit Y. Chap. 2 principes et méthode, in: Baudin F. (ed), *La méthode Rock-Eval®, principes et applications*, ISTE-Wiley, pp. 13–30 (in press).

9 Wattripont A., Bouton N., Espitalie J., Antonas R., Constantinou G. (2018) Rock-Eval sulfur & Geoworks software, in: *Conference Proceedings, First EAGE/IFPEN Conference on Sulfur Risk Management in Exploration and Production*, p. cp-565-00003. https://doi.org/10.3997/2214-4609.201802756.

10 Lever T., Haines P., Rouquerol J., Charsley E.L., van Eckeren P., Burlett D.J. (2014) ICTAC nomenclature of thermal analysis (IUPAC Recommendations 2014), *Pure Appl. Chem.* **86**, 4, 545–553. https://doi.org/10.1515/pac-2012-0609.

11 Henriksen N., Hansen F. (2018) Theories of molecular reaction dynamics, the microscopic foundations of chemical kinetics, 2nd ed., Oxford University Press, ISBN 978-0-19-880501-4.

12 Roduit B. (2000) Computational aspects of kinetic analysis. Part E: The ICTAC kinetics project. Numerical techniques and kinetics of solid state processes, *Thermochim. Acta* **355**, 171–180. https://doi.org/10.1016/S0040-6031(00)00447-0.

13 ASTM E2890-21 (2021) *Standard test method for determination of kinetic parameters and reaction order for thermally unstable materials by differential scanning calorimetry using the Kissinger and Farjas methods.* https://doi.org/10.1520/E2890-21.

14 Webb T.L., Krüger J.E. (1970) Chapter 10 – carbonates, in: McKenzie R.C. (ed), *Differential Thermal Analysis – 1. Fundamental Aspects*, Academic Press, pp. 302–341.

15 Brown W.M., Mackenzie K.J.D., Gainsford G.J. (1984) Thermal decomposition of the basic copper carbonates malachite and azurite, *Thermochim. Acta* **75**, 23–32.

16 Baudin F., Disnar J.R., Aboussou A., Savignac F. (2015) Guidelines for Rock-Eval analysis of recent marine sediments, *Org. Geochem.* **86**, 71–80. https://doi.org/10.1016/j.orggeochem.2015.06.009.

17 Wattripont A., Baudin F., de Rafelis M., Deconinck J.F. (2019) Specifications for carbonate content quantification in recent marine sediments using Rock-Eval pyrolysis, *J. Anal. Appl. Pyrolysis* **140**, 393–403. https://doi.org/10.1016/j.jaap.2019.04.019.

18 Sebag D., Garcin Y., Adatte T., Deschamps P., Ménot G., Verrecchia E.P. (2018) Correction for the siderite effect on Rock-Eval parameters: application to the sediments of Lake Barombi (Southwest Cameroon), *Org. Geochem.* **123**, 126–135. https://doi.org/10.1016/j.orggeochem.2018.05.010.

19 Ordoñez L., Vogel H., Sebag D., Ariztegui D., Adatte T., Russell J.M., Kallmeyer J., Vuillemin A., Friese A., Crowe S. A., Bauer K.W., Simister R., Henny C., Nomosatryo S., The Towuti Drilling Project Scientific Team (2019) Empowering conventional Rock-Eval pyrolysis for organic matter characterization of the siderite-rich sediments of Lake Towuti (Indonesia) using end-member analysis, *Org. Geochem.* **134**, 32–44. https://doi.org/10.1016/j.orggeochem.2019.05.002.

Appendix A

The decomposition curves can be numerically calculated and plotted for given n values and initial weight values. For $n = 0.177$, the curves are displaced in an asymmetrical way towards higher temperatures as the sample weight increases (Fig. 7). Note that the fronting parts of the curves are overlaid, while the tail of the curves are displaced to higher temperatures, as more energy is needed to decompose more carbonate.

For a hypothetical decomposition curve with a reaction order $n = 2$, it is easy to visualize that the curves are displaced in an asymmetrical manner towards lower temperatures and that the temperature at the maximum of thermal decomposition decreases with increasing weights (Fig. A.1A). If $n = 1$, the curves look Gaussian, the temperature at the maximum of thermal decomposition is not dependent of the weight and peaks broaden almost evenly on the front and on the tail side of the almost Gaussian curve (Fig. A.1B). But for $n = 0.9$ or $n = 1.1$, the curves are displaced in a more slightly asymmetrical way, and by eye, it becomes difficult to interpret (Figs. A.1C and A.1D).

In order to infer from curve shapes the order of reaction, one solution would be to divide one curve by another (for instance dividing the curve obtained at 50 mg by the curve obtained with 2 mg of sample). The ratio should be constant (equal to $(50/2)^1 = 25$) if the order of decomposition
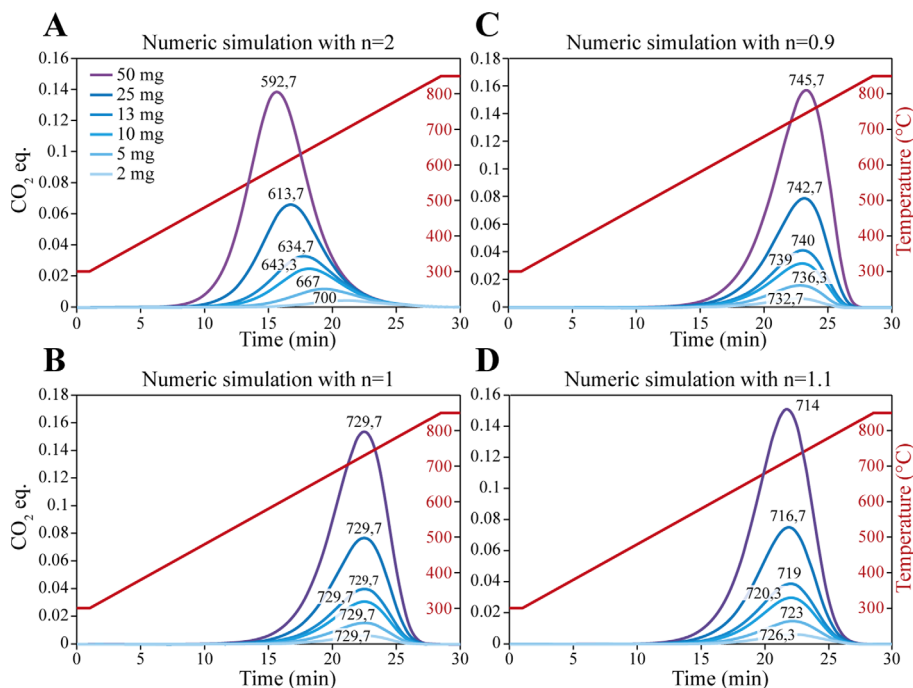

Fig. A.1. Calculated Rock-Eval® thermograms of carbonate thermal decomposition with a given increasing weight and different kinetic orders (n). (A) $n = 2$, (B) $n = 1$, (C) $n = 0.9$ and (D) $n = 1.1$.
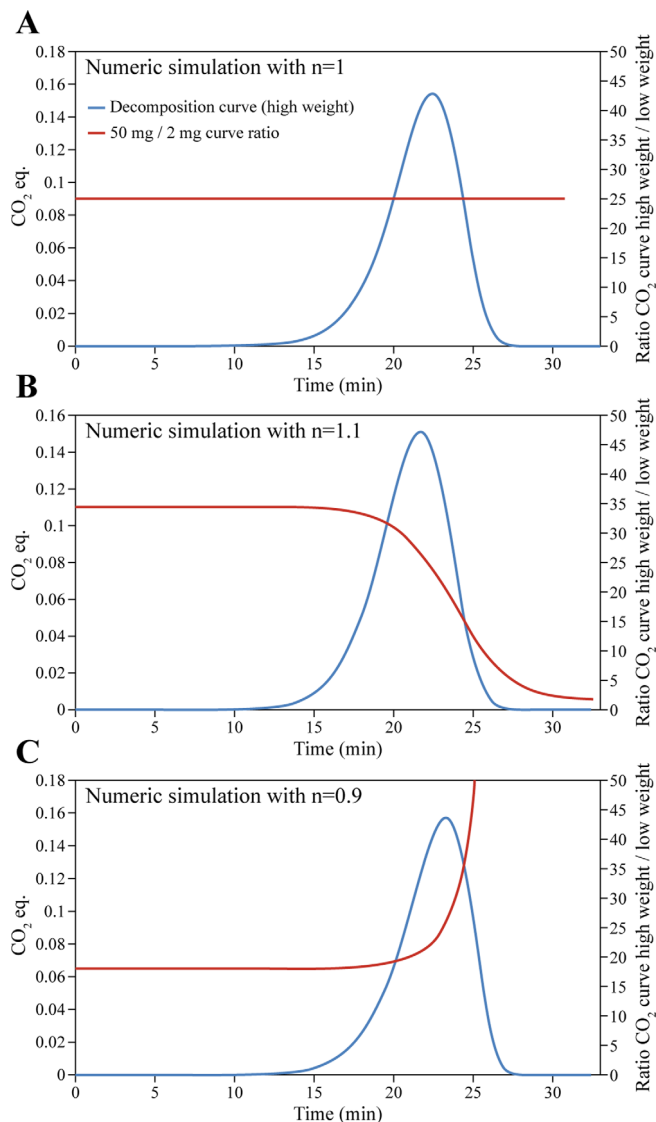
is 1 (Fig. A.2A). If the reaction is of order slightly superior to 1, the curve for high weight is shifted to a lower temperature, and the tailing is lower, thus the ratio high/low weight is decreasing at higher temperature (Fig. A.2B). If the reaction is of order slightly inferior to 1, the curve of high weight is shifted to a higher temperature, and the tailing is higher, thus the ratio high/low weight is increasing at higher temperature (Fig. A.2C). To be noted that the initial ratio is $(50/2)^n$, which gives 18.1 for $n = 0.9$ and 34.5 for $n = 1.1$, is indeed observed on the Figures A.2B and A.2C respectively.

Fig. A.2. Calculated Rock-Eval® thermograms of carbonate thermal decomposition with a weight of 50 mg (blue curve), and calculated curve of the ratio of the decomposition curves of 50 mg divided by 2 mg (red curve), with different kinetic orders (n). (A) $n = 1$, (B) $n = 1.1$ and (C) $n = 0.9$.